Supramolecular self-assembly between symmetric tetramethyl cucurbit[6]uril and dimethylphenylpiperazine hydrochloride

Jian-Hang Hu [a], Zhi-Chao Yu [a], Jia-Yi Zhang [a], Zhi-Nian Liu [a], Run-Xin Hou [a], Yu Xiong [a], Carl Redshaw [b], Zhu Tao [a], Xin Xiao [a, *]

[a] Key Laboratory of Macrocyclic and Supramolecular Chemistry of Guizhou Province, Institute of Applied Chemistry, Guizhou University, Guiyang 550025, China.

E-mail: gyhxxiaoxin@163.com or xxiao@gzu.edu.cn

[b] Department of Chemistry, University of Hull, Hull HU6 7RX, U.K.

Abstract: The interaction between symmetric tetramethyl cucurbit[6]uril (TMeQ[6]) and 2,3-dimethylphenylpiperazine hydrochloride (PMY) has been studied in the presence of $[CdCl_4]^{2-}$. Each port of the TMeQ[6] is connected to PMY through weak interactions such as ion dipole interactions and C-H···O hydrogen bonding interactions, whilst the $[CdCl_4]^{2-}$ is connected with the portal carbonyl oxygen, glycoside urea methylene and a bridging methylene of a TMeQ[6] molecule via ion-dipole interactions. These interactions were evident from a single crystal X-ray diffraction study of TMeQ[6]-PMY-$[CdCl_4]^{2-}$. In addition, the complex can form a one-dimensional supramolecular chain structure, and then assemble into a two-dimensional supramolecular framework, which can be described as a TMeQ[6]-PMY-$[CdCl_4]^{2-}$ based supramolecular framework (QSF).

Keywords: Tetramethyl Cucurbit[6]uril; 2,3-dimethylphenylpiperazine hydrochloride; hydrogen bonding interaction; ion dipole interaction; outer surface interactions.

Introduction

Supramolecular self-assembly has received intense interest recently given its applications in areas including chemistry [1-6], materials [7,8], environmental science [9-11], and life science [12,13]. An essential step in the process of creating new systems is the selection of diverse building blocks, which allow for the creation of supramolecular self-assembled systems with unique shapes and distinct features stabilized through weak interactions such as ion-ion dipoles and intermolecular hydrogen bonds.

Crown ethers, cyclodextrins and calixarenes are examples of synthetic macrocyclic molecules, and in recent years cucurbit[*n*]uril (Q[*n*] or CB[*n*]) have also been added to this family. Studies on common cucurbit[*n*]urils and their uses have suffered due to poor solubility in aqueous and organic phases. As a result, increasing the solubility of cucurbit[*n*]urils has attracted attention, and over time, several substituted cucurbit[*n*]urils have appeared with enhanced solubility. [14] Fully substituted cyclohexyl cucurbit[*n*]uril (n = 5, 6) [15], which are soluble in alcohol-water systems, were first discovered in 2001 by Kim *et al*. The number of modified Q[*n*]s has expanded in recent years, with studies mostly concentrating on methyl-, [16,17] hydroxyl-, [18] cyclopentyl-, [19] cyclohexyl- [20] substituted Q[*n*]s. Such work served as the starting point for further studies on cucurbit[*n*]uril-based polymers. One of the methyl substituted cucurbit[*n*]urils is the symmetric tetramethyl cucurbit[6]uril (TMeQ[6]), which is structurally similar to cucurbit[6]uril, but has four additional substituted methyl groups on the waist. It is generally known that cucurbit[6]uril is notorious for being difficult to dissolve in water, however the addition of the four methyl groups significantly increases its solubility, making further practical work more favorable.

Since 2014, our research group and others have been developing Q[*n*]-based supramolecular frameworks based on OSIQs. [21-27] The outer surface interactions of Q[*n*]s (OSIQs) were first hypothesized by us [21], specifically self- and anion-induced OSIQs [22], which involved the positively charged outer surface of Q[*n*]s. More investigation has revealed that Q[*n*]-based coordination polymers and frameworks can be used to recover a wide range of metal ions [26,27], as well as to prepare different sensors [28-36].

Building supramolecular organic frameworks with structural properties based on weak intermolecular interactions, such as hydrogen bonds, ion-dipole interactions, C-H contacts, and other interactions, has become popular over the past ten years [37]. Supramolecular organic frameworks (SOFs), which get their driving force from supramolecular interactions, are frequently easy to make and have strong reversibility. However, SOFs frequently fall short in terms of strength and stability. In order to avoid these problems, choosing organic building components with solid structures while creating SOFs may be a good solution [37,38]. In fact, the influence of the surface on a Q[*n*]-based supramolecular framework (QSF) can make the process easier and more effective [25]. A Q[*n*] at the outer surface has a positive electrostatic potential, which is where the driving force comes from. Based on the many species interacting with the outer surface of Q[*n*]s, the QSF assembly process may be broadly divided into three types: self-induced, anion-induced, and aromatic-ring-induced (termed aromatic-induced hereafter).

2,3-Dimethylphenylpiperazine hydrochloride (PMY) is a member of the phenyl piperazines. It is employed in a crucial step in the production of receptor antagonists. Phenylpiperazines exhibit good receptor subtype selectivity and urinary tract tissue selectivity, according to studies. Studies on the structure-activity relationship (SAR) of phenylpiperazines have demonstrated this type of compound's ability to inhibit $\alpha1$ receptor and 5-HT receptor in recent years [39,40]; the phenylpiperazine part is α_1. In studies where receptors bind to drug basic centers, phenylpiperazine can be connected to carriers like anti-heterocyclic rings to give compounds with distinctive pharmacological properties, which can afford control of neuro-drugs and anti-virus agents [41-45]. Consequently, the study of this family of chemicals has gained popularity.

In this study, the piperazine ring interacts with the outer surface of TMeQ[6] to form a supramolecular self-assembly framework using PMY as the guest molecule and TMeQ[6] as the host; Figure 1 depicts the structures of TMeQ[6] and PMY. We have employed ^{1}H NMR spectroscopy and single crystal X-ray diffraction, and report how a supramolecular self-assembled frame was created to model the interactions between the piperazine and cucurbit[*n*]uril at the surface.

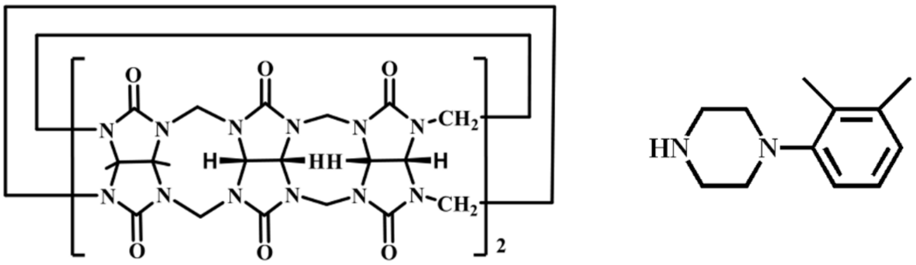

TMeQ[6] **PMY**

Figure 1. Structures of TMeQ[6] and PMY.

Experimental section

Materials and instruments

PMY was purchased from Aladdin (Shanghai, China) and used as supplied without further purification. TMeQ[6] was prepared according to the literature method [46]. A JEOL JNM-ECZ400S nuclear magnetic resonance spectrometer (Japan Electronics Corporation, 400 MHz) was used to record the ^{1}H NMR spectra. Fluorescence emission spectra were recorded on a VARIAN Cary Eclipse spectrofluorometer (Varian, Inc., Palo Alto, CA, USA). The crystal structure was determined using data collected using a Bruker D8 venture single crystal diffractometer.

Experimental methods

2.1 Single-crystal X-ray crystallography

The crystal structure of TMeQ[6]-PMY-$[CdCl_4]^{2-}$ was ascertained using data obtained from a Bruker D8 venture single crystal diffractometer. By evaporating the solvent, a single crystal was created from a 3M HCl solution. A graphite monochromator was used, together with a Mo K radiation source (λ = 0.71073 Å), a temperature of 298.15 K, and the f and ω Scans mode. The SAINT program was used to adjust the data for the polarization and Lorentz effects, and SADABS was used to apply a semi-empirical absorption correction based on comparable reflections. The structure was solved using dual space methods in SHELXT, and then was refined using SHELXL-2018 [47,48] implemented within Olex2 [49]. Anisotropic displacement parameters were used to tune all of the non-hydrogen atoms in the primary molecules. Hydrogen atoms bonded to carbon were added to the computation position and treated as riding atoms. The isotropic displacement parameters of the parent atom are 1.2 times greater than those of the child atom. Table 1 lists the crystal parameters, data collection options, and refinement statistics. The crystal data has been deposited at the Cambridge crystal data center (CCDC-2207701). These data can be obtained free of charge via www.ccdc.cam.ac.uk/data_request/cif, by emailing data_request@ccdc.cam.ac.uk, or by contacting The Cambridge Crystallographic Data Centre, 12, Union Road, Cambridge CB21EZ, UK (fax: +44 1223-336033).

2.2 ^{1}H NMR measurements

The ^{1}H NMR spectra were recorded at 298.15K. D_2O was used for the field frequency lock.

2.3 Preparation of complex TMeQ[6]-PMY-$[CdCl_4]^{2-}$

To a solution of PMY (10 mg, 0.044 mmol) in 3 ml of 3M HCl, TMeQ[6] (10 mg, 0.010 mmol) was added, then $CdCl_2 \cdot 2.5\ H_2O$ (10 mg, 0.044 mmol) was also added to this solution. The mixture was heated until it is completely dissolved. The filtrate was evaporated slowly under air for about a week, and diamond red crystals of the compound TMeQ[6]-PMY-$[CdCl_4]^{2-}$ were obtained in a yield of 2.6 mg (23%).

Results and discussion

Symmetric tetramethyl cucurbit[6]uril-based supramolecular frameworks

TMeQ[6]-PMY: Crystal Data for $C_{64}H_{84}Cd_2Cl_8N_{28}O_{18}$ (M =2041.99 g/mol): triclinic, space group P-1. Following the preparation outlined in the experimental section, colorless crystals were obtained. The crystal structure is shown in Fig. 2 and all measured distances are based on the interaction between hydrogen atoms and receptors. A Q[*n*] can be used to build different kinds of supramolecular framework materials with varied structural properties since it has outer surface interactions with a positive electrostatic potential. QSFs can develop in three different ways: on their own, when exposed to inorganic anions, and when exposed to organic aromatic molecules.

Organic aromatics interact with the positive electrostatic potential OSIQ through hydrogen bonding, C-H···π, C-H···O, and ion-ion dipole interactions to generate a variety of QSFs. Herein, we describe the synthesis of a TMeQ[6]-based QSF two-dimensional structure using 2,3-dimethylphenyl-piperazine hydrochloride (PMY) as a structure guiding agent. We have concentrated on inorganic anion-induced QSFs caused by aromatic organic chemicals and TMeQ[6]. According to crystal data, the piperazine ring on PMY interacts with the Cl^- on the $[CdCl_4]^{2-}$ anion to generate a C-H···Cl^- contact as well as the carbonyl carbon of TMeQ[6] to form an ion dipole interaction. We discovered that six anions, three of which have bond lengths of 2.930 Å, 3.227 Å, 3.375 Å, and 2.941 Å, formed in pairs and resided around the outside of a single TMeQ[6]. The remaining three anions are symmetrical and have the same bond length (Fig. 2b). We removed $[CdCl_4]^{2-}$ to make the visualization easier, and the two PMY molecules interact with the identical TMeQ[6] molecule (figure 2c). This is in line with the QSF that the aforementioned aromatic chemical substances caused. We choose here only one end for investigation because the interaction mechanisms of the upper and lower PMY and TMeQ[6] ports are identical. Figure 2c illustrates the weak intermolecular interactions that PMY and TMeQ[6] carbonyl oxygen and carbonyl carbon create. In a clockwise direction, their bond lengths are 2.605 Å, 2.566 Å, 2.231 Å, 2.248 Å, 2.569 Å, 2.438 Å, 2.632 Å, and 2.338 Å, respectively; the interaction is C-H···O.

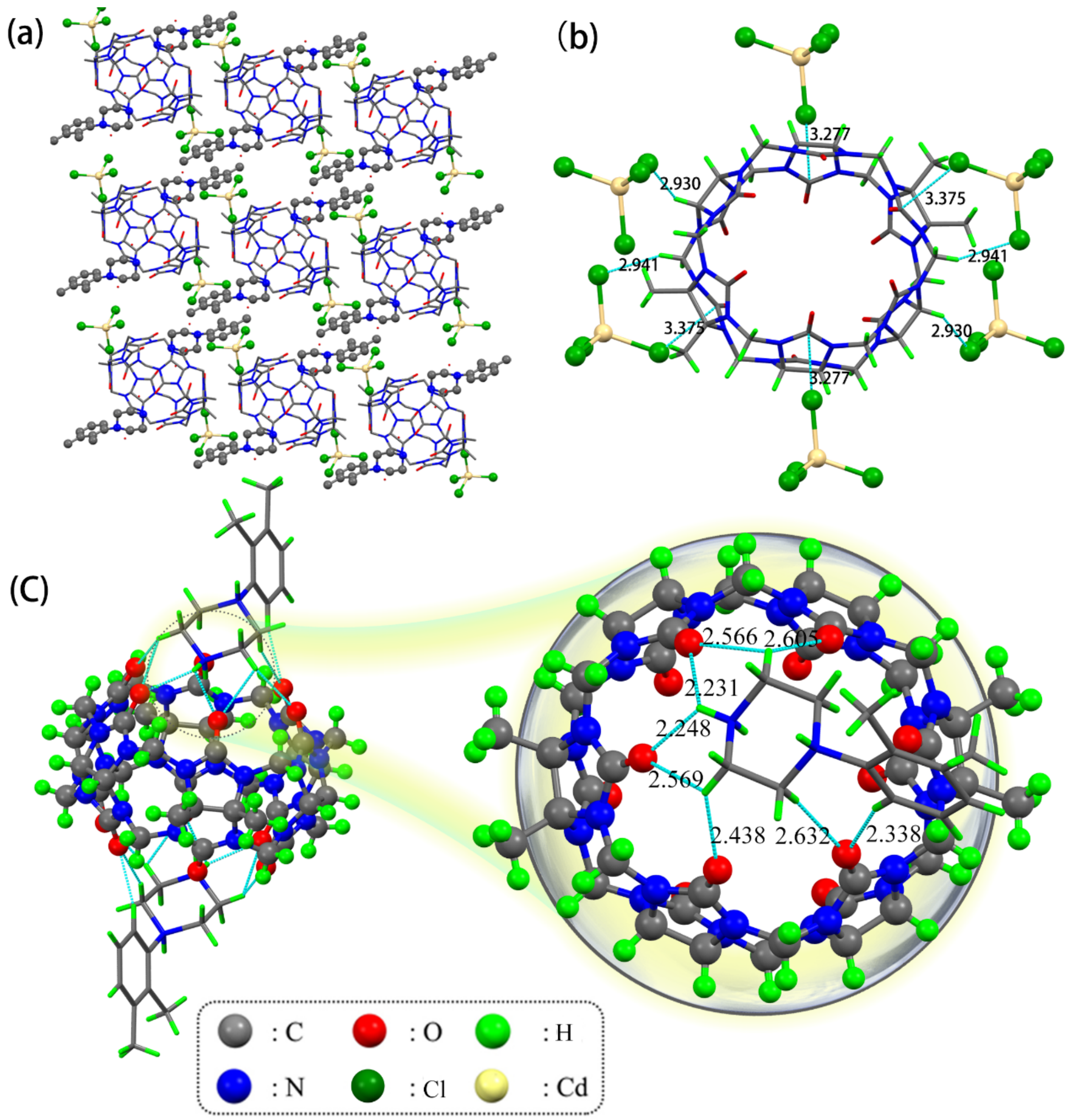

Figure 2. (a) Overall-view of the crystal structure of TMeQ[6]-PMY-$[CdCl_4]^{2-}$; (b) The crystal structure of TMeQ[6]-$[CdCl_4]^{2-}$; (c) The crystal structure of TMeQ[6]-PMY. The structures shown in figure 2b and 2c are part of the same structure only with either $[CdCl_4]^{2-}$ or PMY omitted for clarity.

The fundamental component of the TMeQ[6]-based QSF is shown in Figure 3a, which was created by the interaction of one TMeQ[6] molecule with two PMY. Additionally, each PMY unit interacts with a TMeQ[6], but it also forms a one-dimensional supramolecular chain structure with a C-H bond length of 2.834 Å with nearby TMeQ[6] units as shown in Fig. 3b. Moreover, there are π - π stacking interactions between the two PMY aromatic rings belonging to different TMeQ[6] units (see Fig. S4, SI). Additionally, by encasing both ends of the one-dimensional supramolecular chain, the assembly transforms the TMeQ[6] port into a conventional two-dimensional layered structure (Fig. 3c).

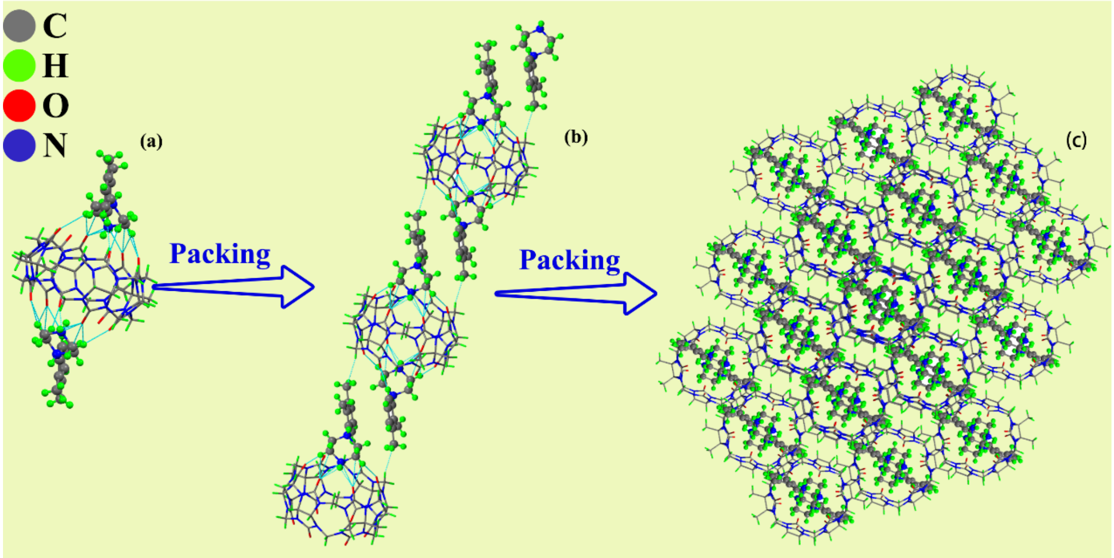

Figure 3. TMeQ[6]-PMY outer surface interactions.

In addition to interactions with nearby aromatic organic compounds, the Q[*n*]'s positive electrostatic potential outer surface contacts can also occur with negatively charged species (especially anions). When the right circumstances are present, Q[*n*] molecules and anions easily form QSFs. For example, when metal ions are added to the Q[*n*]-PMY system, polychlorinated metal anions are easily formed.

As seen in Figure 4a, the ionic dipole interactions between the portal carbonyl, aglycone methyl, and bridging methylene of TMeQ[6] molecule allows for the connection of $[CdCl_4]^{2-}$. Six $[CdCl_4]^{2-}$ anions surround each TMeQ[6] molecule, as is shown in the figure. The Q[*n*]s gateway carbonyl oxygen can connect with the positive electrostatic potential outside wall of nearby Q[*n*]s through dipole interactions to generate different QSFs in addition to the aforementioned two types of outer surface Q[*n*] contacts. These outcomes include interactions between the portal carbonyl oxygen atom of a Q[*n*] molecule and the methine unit of a neighboring Q[*n*], a bridging methylene unit, and the portal carbonyl carbon atoms' dipole interactions (figure 4b).

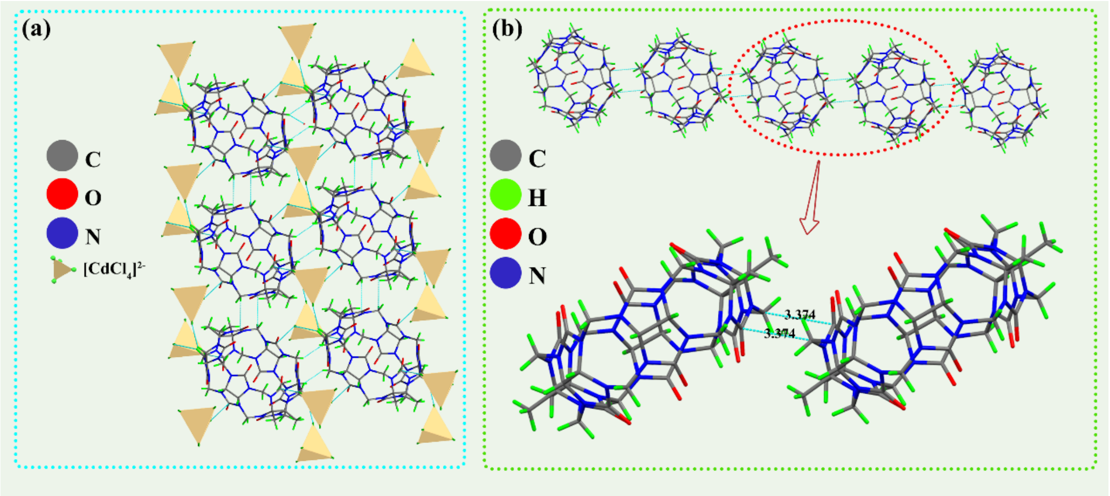

Figure 4. (a) The TMeQ[6]-$[CdCl_4]^{2-}$ interactions; and (b) Self-induced TMeQ[6]-TMeQ[6].

In the case of the NMR data, after adding TMeQ[6] to the PMY D_2O solution, Fig. 5 and S6 demonstrates that the methylene peaks H_c and H_d on the piperazine ring of PMY experienced an obvious down-field movement, with the corresponding chemical shift values changing from 2.85 ppm and 3.1 ppm to 3.0 ppm and 3.3 ppm, respectively. At the same time, the other proton resonance peaks of PMY also exhibit slight down-field chemical shifts. These phenomena indicate that the PMY molecule is located outside the TMeQ[6], and the piperazine ring of PMY is located at the port of TMeQ[6]. This is consistent with the solid-state crystal structure data.

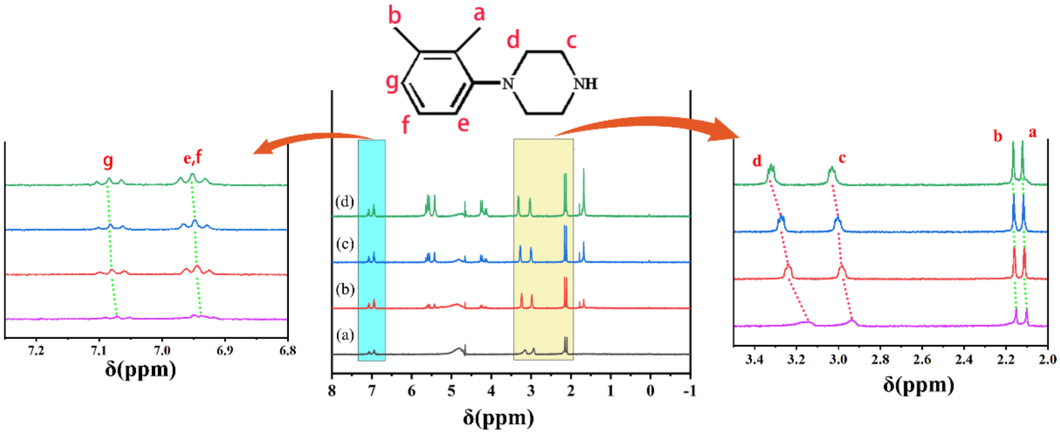

Figure 5. ^1H NMR spectra (400 MHz, D_2O) of PMY and the presence of TMeQ[6] (a) 0 equiv.; (b) 1.00 equiv.; (c) 1.50 equiv.; (d) 2.00 equiv.

Conclusion

In short, we discovered that in an acidic solution, a supramolecular self-assembly was formed between symmetric tetramethyl cucurbit[6]uril and dimethyl phenylpiperazine hydrochloride via multiple non-covalent interactions. A number of methods, including X-ray crystallography, ^{1}H NMR spectroscopy have been employed to characterize the system. This work shows that the driving force for the formation of the TMeQ[6]-based supramolecular frameworks (TMeQ[6]-PMY-$[CdCl_4]^{2-}$) is the weak interactions between the guest and host, such as C-H···O, and the ion-dipole interactions between the inorganic metal anions and host-guest.

Acknowledgments

This work was financially supported by the Science and Technology Fund of Guizhou Province (No.). CR thanks the University of Hull for support.

Conflict of Interest

There is no conflict of interest.

References

[1] K. M. Park, J. Murray and K. Kim, Ultrastable Artificial Binding Pairs as a Supramolecular Latching System: A Next Generation Chemical Tool for Proteomics, Acc. Chem. Res. 2017, 50, 644-646.

[2] X.-K. Fang, P. Kögerler, L. Isaacs, S. Uchida, N. Mizuno. Cucurbit[n]uril-Polyoxoanion Hybrids. J. Am. Chem. Soc., 2009, 131, 432-433.

[3] J. Murray, K. Kim, T. Ogoshi, W. Yao and B. C. Gibb, The aqueous supramolecular chemistry of cucurbit[n]urils, pillar[n]arenes and deep-cavity cavitands, Chem Soc. Rev., 2017, 46, 2479-2496.

[4] D. Shetty, J. K. Khedkar, K. M. Park and K. Kim, Can we beat the biotin–avidin pair?: cucurbit[7]uril-based ultrahigh affinity host–guest complexes and their applications, Chem. Soc. Rev., 2015,44, 8747-8761.

[5] M. Liu, R. Cen, J.-S. Li, Q. Li, Z. Tao, X. Xiao, and L. Isaacs, Double-Cavity Nor-Seco-Cucurbit[10]uril Enables Efficient and Rapid Separation of Pyridine from Mixtures of Toluene, Benzene, and Pyridine, Angew. Chem. Int. Ed. 2022, e202207209.

[6] H.-G. Nie, Z. Wei, X.-L. Ni, and Y. Liu, Assembly and Applications of Macrocyclic-Confinement-Derived Supramolecular Organic Luminescent Emissions from Cucurbiturils, Chem. Rev. 2022, 122, 9, 9032–9077.

[7] J. Liu, Y. Lan, Z.-Y. Yu, Cindy S.Y. Tan, R. M. Parker, C. Abell and O. A. Scherman, Cucurbit[n]uril-Based Microcapsules Self-Assembled within Microfluidic Droplets: A Versatile Approach for Supramolecular Architectures and Materials, Acc. Chem. Res. 2017, 50, 208–217.

[8] K. I. Assaf, W. M. Nau. Cucurbiturils: from synthesis to high-affinity binding and catalysis. Chem. Soc. Rev., 2015, 44 (2), 394-418.

[9] I. Hwang, W. S. Jeon, H.-J. Kim, D. Kim, H. Kim, N. Selvapalam, N. Fujita, S. Shinkai, K. Kim. Cucurbit[7]uril: A Simple Macrocyclic, pH-Hydrogelator Exhibiting Guest-Induced Stimuli-Responsive Behavior. Angew. Chem. Int. Ed., 2007, 46, 210-213.

[10] W. Zhang, Y. Luo, J. Zhao, C. Zhang, X.-L. Ni, Z. Tao and X. Xiao, Controllable fabrication of a supramolecular polymer incorporating twisted cucurbit[14]uril and cucurbit[8]uril via self-sorting, Chin. Chem. Lett., 2022, 33, 2455-2458.

[11] K.-N. Wei, G.-X. Song, S.-Z. Huang, Q. Tang, J.-H. Hu, Z. Tao and Y. Huang, Lab-on-a-Molecule Probe: Multitarget Detection of Five Aromatic Pesticides Using a Supramolecular Probe under Single Wavelength Excitation, J. Agric. Food Chem., 2022, 70, 5784−5793.

[12] Tami A. Martyn, Jason L. Moore, Ronald L. Halterman, and Wai Tak Yip. Cucurbit[7]uril Induces Superior Probe Performance for Single-Molecule Detection. J. Am. Chem. Soc., 2007, 129, 34, 10338–10339.

[13] C. Sun, Z.-Y. Wang, L.-D. Yue, Q.-X. Huang, Q. Cheng, R.-B. Wang. Supramolecular Induction of Mitochondrial Aggregation and Fusion. J. Am. Chem. Soc., 2020, 142, 16523-16527.

[14] R.-L. Lin, J.-X. Liu, K. Chen and C. Redshaw, Supramolecular chemistry of substituted cucurbit[*n*]urils, Inorg. Chem. Front., 2020, 7, 3217-3246.

[15] J. Zhao, H.-J. Kim, J. Oh, S.-Y. Kim, J.-W. Lee, S. Sakamoto, K. Yamaguchi and K. Kim, Cucurbit[*n*]uril Derivatives Soluble in Water and Organic Solvents, Angew. Chem., 2001, 113, 4363-4365.

[16] Y. Zhao, S.-F. Xue, Q.-J. Zhu, Z. Tao, J. Zhang, Z. Wei, L. Long, M. Hu, H. Xiao and A. Day, Synthesis of a symmetrical tetrasubstituted cucurbit[6]uril and its host-guest inclusion complex with 2,2′-bipyridine, Chin. Sci. Bull., 2004, 49, 1111-1116.

[17] B. Vinciguerra, P. Y. Zavalij and L. Isaacs, Synthesis and Recognition Properties of Cucurbit[8]uril Derivatives, Org. Lett., 2015, 17, 5068−5071.

[18] M.-M. Ayhan, H. Karoui, M. Hardy, A. Rockenbauer, L. Charles, R. Rosas, K. Udachin, P. Tordo, D. Bardelang and O. Ouari, Comprehensive Synthesis of Monohydroxy-Cucurbit[*n*]urils (n=5,6,7,8): High Purity and High Conversions, J. Am. Chem. Soc., 2015, 137, 10238-10245.

[19] F. Wu, L.-H. Wu, X. Xiao, Y.-Q. Zhang, S.-F. Xue, Z. Tao and A. Day, Locating the Cyclopentano Cousins of the Cucurbit[*n*]uril Family, J. Org. Chem., 2012, 77, 606-611.

[20] L. Zheng, J. Zhu, Y. Zhang, Qi. Zhu, S.-F. Xue, Z. Tao, J. Zhang, X. Zhou, Z. Wei, L. Long and A. Day, Opposing substitution in cucurbit[6]urils forms ellipsoid cavities: the symmetrical dicyclohexanocucurbit[6]uril is no exception highlighted by inclusion and exclusion complexes, Supramol. Chem., 2008, 20, 709−716.

[21] X.-L. Ni, X. Xiao, H. Cong, Q.-J. Zhu, S.-F. Xue and Z. Tao. Self-assemblies based on the "outer-surface interactions" of cucurbit[n]urils: new opportunities for supramolecular architectures and materials. Acc. Chem. Res., 2014, 47, 1386-1395.

[22] Y. Huang, R.-H. Gao, M. Liu, L.-X. Chen, X.-L. Ni, X. Xiao, H. Cong, Q.-J. Zhu, K. Chen and Z. Tao. Cucurbit[n]uril-Based Supramolecular Frameworks Assembled through Outer-Surface Interactions. Angew. Chem. Int. Ed., 2021, 60, 15166-15191.

[23] I. Hwang, W. S. Jeon, H.-J. Kim, D. Kim, H. Kim, N. Selvapalam, N. Fujita, S. Shinkai and K. Kim. Cucurbit[7]uril: A Simple Macrocyclic, pH-Hydrogelator Exhibiting Guest-Induced Stimuli-Responsive Behavior. Angew. Chem. Int. Ed., 2007, 46, 210-213.

[24] K. I. Assaf and W. M. Nau. The chaotropic effect as an assembly motif in chemistry. Angew. Chem. Int. Ed., 2018, 57, 13968-13981.

[25] X.-K. Fang, P. Kögerler, L. Isaacs, S. Uchida and N. Mizuno. Cucurbit[n]uril-Polyoxoanion Hybrids. J. Am. Chem. Soc., 2009, 131, 432-433.

[26] Y.-Q. Yao, Y.-J. Zhang, C. Huang, Q.-J. Zhu, Z. Tao, X.-L. Ni and G. Wei. Cucurbit[10]uril-based smart supramolecular organic frameworks in selective isolation of metal cations. Chem. Mater., 2017, 39, 5468–5472.

[27] L.-X. Chen, M. Liu, Y.-Q. Zhang, Q.-J. Zhu, J.-X. Liu, B.-X. Zhu and Z. Tao. Outer surface interactions to drive cucurbit[8]uril-based supramolecular frameworks: possible application in gold recovery. Chem. Commun., 2019, 55, 14271-14274.

[28] J. Yu, H. Wang, Y. Liu. Double-Network Confined Supramolecular Phosphorescence Light-Harvesting Boosting Photocatalysis. Adv. Optical Mater., 2022, 2201761.

[29] A. C. Garcia, L. N. Zakharov, and Mi. D. Pluth. Supramolecular Activation of S8 by Cucurbiturils in Water and Mechanism of Reduction to H2S by Thiols: Insights into Biological Sulfane Sulfur Trafficking. J. Am. Chem. Soc., 2022 144 (33), 15324-15332.

[30] H. Wu, L. O. Jones, Y. Wang, D.-K. Shen, Z.-C. Liu, L. Zhang, K. Cai, Y. Jiao, C. L. Stern, G. C. Schatz, and J. F. Stoddart. High-Efficiency Gold Recovery Using Cucurbit[6]uril. ACS Appl. Mater. Interfaces, 2020, 12, 34, 38768–38777

[31] A. I. Lazar, F. Biedermann, K. R. Mustafina, K. I. Assaf, A. Hennig, and W. M. Nau. Nanomolar Binding of Steroids to Cucurbit[n]urils: Selectivity and Applications. J. Am. Chem. Soc., 2016, 138, 39, 13022–13029.

[32] H. Wu, J. Zhao, X.-N. Yang, D. Yang, L.-X. Chen, C. Redshaw, L.-G. Yang, Z. Tao and X. Xiao. A cucurbit[8]uril-based probe for the detection of the pesticide tricyclazole, Dyes and Pigments, 2022, 199, 110076.

[33] C. Sun, Z.-Y. Wang, L.-D. Yue, Q.-X. Huang, Q. Cheng and R.-B. Wang. Supramolecular Induction of Mitochondrial Aggregation and Fusion. J. Am. Chem. Soc., 2020, 142, 16523-16527.

[34] S.-W. Guo, Q.-X. Huang, Y. Chen, J.-W. Wei, J. Zheng, L.-Y. Wang, Y.-T. Wang and R.-B. Wang. Synthesis and Bioactivity of Guanidinium-Functionalized Pillar[5]arene as a Biofilm Disruptor. Angew. Chem. Int. Ed., 2021, 60, 618-623.

[35] W. Zhang, Y. Luo, Y. Zhou, M. Liu, W.-T. Xu, B. Bian, Z. Tao, X. Xiao, A highly selective fluorescent chemosensor probe for detection of Fe^{3+} and Ag^{+} based on

supramolecular assembly of cucurbit[10]uril with a pyrene derivative, Dyes and Pigments, 2020, 176, 108235, ISSN0143-7208.

[36] W. Zhang, Y. Luo, J. Zhao, C. Zhang, X.-L. Ni, Z. Tao and X. Xiao, Controllable fabrication of a supramolecular polymer incorporating twisted cucurbit[14]uril and cucurbit[8]uril via self-sorting, Chin. Chem. Lett., 2022, 33, 2455-2458,ISSN 1001-8417,https://doi.org/10.1016/j.cclet.2021.11.053.

[37] W.-B. Yang, A. Greenaway, X. Lin, R. Matsuda, A. J. Blake, C. Wilson, W. Lewis, P. Hubberstey, S. Kitagawa, N. R. Champness, M. Schröder. Exceptional thermal stability in a supramolecular organic framework: porosity and gas storage. J. Am. Chem. Soc., 2010, 132, 14457-14469.

[38] I. Hisaki, Y. Suzuki, E. Gomez, B. Cohen, N. Tohnai and A. Douhal. Docking strategy to construct thermostable, single-crystalline, hydrogen-bonded organic framework with high surface area. Angew. Chem. Int. Ed., 2018, 57: 12650-12655.

[39] F.-Y. Tian, R.-X. Cheng, Y.-Q. Zhang, Z. Tao and Q.-J. Zhu. Synthesis, Adsorption, and Recognition Properties of a Solid Symmetric Tetramethylcucurbit[6]uril-Based Porous Supramolecular Framework. Aust. J. Chem, 2020, 9619461, 10 pages. https://doi.org/10.1155/2020/9619461

[40] R.-X. Cheng, F.-Y. Tian, Y.-Q. Zhang, K. Chen, Q.-Jiang Zhu and Z. Tao. TMeQ[6]-based supramolecular frameworks assembled through outer surface interactions and their potential applications. J. Mater. Sci., 2020, 55, 16497-16509.

[41] M. L. López-Rodríguez, M. L. Rosado, B. Benhamú, M. J. Morcillo, E. Fernández and K.-J. Schaper. Synthesis and Structure−Activity Relationships of a New Model of Arylpiperazines. 2. Three-Dimensional Quantitative Structure−Activity Relationships of Hydantoin−Phenylpiperazine Derivatives with Affinity for 5-HT$_{1A}$ and α_1 Receptors. A Comparison of CoMFA Models. J. Med. Chem.,1997, 40, 1648-1656.

[42] Y.-X. Sui, A. -S. Sun, L.-M. Yu, Q. Wu, X. -N. Huang, J. -S. Shi and Y. Mu. Effects of naftopidil derivative BWYJ on blood pressure in rats and hemodynamics in cats. Chinese Clinical Pharmacology and Therapeutics, 2005, 10, 852-856.

[43] J.-L. Pan, L. Tao and Y. Xing. Synthesis of N-phenylpiperazine. Chinese Journal of Modern Applied Pharmacy, 2001, 18, 372-374.

[44] X. He, Z.-Y. Lin and L.-Y. Zhu. Cinnamamide and α Synthesis and vasodilatory activity of phenyl cinnamamide derivatives. Pharm. J.,1999, 34, 192-196.

[45] B.-Q. Bai, M. Yuan and X. Zhou. Synthesis of 1 - (2,3-dimethylphenyl) piperazine. Journal of Guangzhou Medical College, 2007, 35, 54-56.

[46] Y.-J. Zhao, S.-F. Xue, Q.-J. Zhu, Z. Tao, J.-X. Zhang, Z.-B. Wei, L.-S. Long, M.-L. Hu, H.-P. Xiao and A. I. Day, Chin. Sci. Bull., 2004, 49, 1111.

[47] G.M. Sheldrick, Acta Crystallogr. Sect. A., 2008, 64,112–122.

[48] G.M. Sheldrick, Crystal structure refinement with SHELXL, Acta Cryst., 2015, C71, 3–8.

[49] O.V. Dolomanov, L.J. Bourhis, R.J. Gildea, J.A.K. Howard, H. Puschmann, OLEX2: a complete structure solution, refinement and analysis program, J. Appl. Cryst., 2009, 42, 339–341.